

# MODIFICATION OF WATER AFFINITY ON THE SURFACE OF CERAMIC CONSTRUCTION SUBSTRATES FOR SELF-CLEANING APPLICATIONS

**Oswaldo Saucedo Orozco<sup>a</sup>, Juan Jacobo Ruiz Valdés<sup>a,b</sup>, Andrea Quetzalli Cerdán Pasarán<sup>a</sup>, Astrid Iriana Sánchez Vázquez<sup>a</sup>, Juan Manuel Hernández López<sup>a</sup>, Teresa Montalvo<sup>a</sup>, Fernando Lozano Assad<sup>b</sup>.**

<sup>a</sup> **Universidad Autónoma de Nuevo León, Faculty of Chemical Sciences - Mexico**

<sup>b</sup> **Tile Council of North America – Mexico.**

## 1. INTRODUCTION

Over the years, one of the perennial problems facing construction elements is the degradation of the materials they are composed of. This phenomenon is caused by a number of factors, including moisture on the surface of construction elements, exposure to certain environmental pollutants, and the action of biological agents. Degradation can manifest itself in various ways, such as the blackening of surfaces, growth of micro-organisms, or even the appearance of fractures and detachment of the outer surface layers of structures. Such phenomena not only affect the aesthetic appearance of buildings but also pose risks to the health and safety of people in the affected areas. To combat these problems, it is essential to carry out both preventive and corrective maintenance [1]-[3].

In an effort to reduce maintenance costs and prolong the life span of buildings, numerous studies have been conducted in recent decades focusing on the development and application of coatings that affect how the surface of the material interacts with water. Such coatings can render materials hydrophobic or hydrophilic via a number of techniques [4]-[8].

The two leading ways to modify the water affinity of materials are: 1) by making changes to surface roughness, thus generating hierarchical structures of micro- and nanometric roughness on the surface to reduce the contact area between liquid and materials, using oxides such as  $\text{SiO}_2$  [9]-[13],  $\text{ZnO}$  [14]-[16],  $\text{TiO}_2$  [17]-[19] and  $\text{Al}_2\text{O}_3$  [20], [21], among others; 2) by incorporating functional groups onto the surface of the material, such as compounds with long-chain aliphatic groups to increase water repellency and OH groups to increase water affinity.

Among the metal oxides most commonly cited in the literature used to alter surface roughness are  $\text{SiO}_2$ ,  $\text{TiO}_2$  and  $\text{ZnO}$ . These oxides can be used in the form of commercially available nanoparticles in powder or in both hydrophobic and hydrophilic solutions. It is also possible to prepare nanoparticles by sol-gel reactions using various routes and precursors, which enables a variety of surface performance characteristics to be achieved once they are deposited on the relevant substrates.

A prominent example is the work of Wang [4], who describes a super-hydrophilic coating fabricated by mixing two  $\text{SiO}_2$  sol-gel solutions, one obtained using an acid catalyst and the other an alkaline one. The first type of sol produces a dense coating with good mechanical stability, while the second type allows very high transmittance to be achieved. The results of his study revealed an average contact angle of  $4.6^\circ$  and an increase in transmittance of the original glass substrate from 88.1% to 94.45% for the glass substrate with the new coating. Furthermore, the coating is reported to exhibit satisfactory mechanical strength, which was verified by pencil hardness tests.

Another author reporting a  $\text{SiO}_2$  coating with good mechanical stability is Zhao [22]. In his research, he developed super-hydrophobic surfaces on various substrates such as wood, copper plates, pieces of fabric, Mg-Al alloys and silicon wafers, with contact angle values of up to  $163^\circ$ . In addition, he demonstrated this mechanical stability by abrasion testing.

The above examples highlight the versatility of coatings based on nanoparticles and metal oxides to modify surface properties, which has significant applications in various areas of science and technology.

The use of  $\text{TiO}_2$  and  $\text{ZnO}$  not only provides super-hydrophobic and super-hydrophilic properties but is also able to degrade organic pollutants by UV/visible light irradiation, which has resulted in significant advances in research. In Wang's work [5], degradation of the pollutant methyl orange was achieved by generating a coating from  $\text{TiO}_2$  nanoparticles deposited on  $\text{SiO}_2$  microspheres. This superhydrophobic coating proved effective in degrading pollutants under the influence of UV/visible light.

In addition, Talinungsang et al [23] developed a super-hydrophilic coating combining  $\text{ZnO}$  and  $\text{SnO}_2$ . This coating displayed effective photocatalytic properties for degrading methyl orange and methylene blue, while they also explored coverings that are able to alter wettability by activation with ultraviolet light.

Rodriguez-Villalobos [16] presented an interesting study on the development of a coating made with  $\text{ZnO}$  nanorods with hydrophilic properties on marble and natural stone substrates.

When the coated pieces were exposed to UV light for one hour, a significant change in contact angle was observed, which decreased from close to 20° and 10° to below 5°. This method of activation with UV displays a promising ability to alter surface properties dynamically.

In another study, Jingpeng Li [24] presented a ZnO- and OTS-based coating on bamboo substrates. In his work, tests were carried out to alter the contact angle by irradiation with UV light for 12 hours, achieving values close to 0°. Subsequently, the pieces were kept in the dark for 10 days, which produced contact angles of up to 153°.

Such advances in the application of TiO<sub>2</sub> and ZnO, not only to modify surface wettability but also to degrade organic pollutants through photocatalysis, open up fresh opportunities for developing coatings and technologies that may have a significant impact in various areas of science and technology.

The main objective of our research is to modify water affinity on the surface of different ceramic substrates used in construction. That would allow such coatings to be applied on the surfaces of buildings and items of cultural value, such as monuments and historic edifices, to prolong their useful life, preserve cultural heritage and reduce the constant need for maintenance, as well as the high costs associated with those tasks.

## 2. METHOD

Two types of coating have been developed in our study: a hydrophobic one using SiO<sub>2</sub> nanoparticles and triethoxyoctylsilane (TOS) in solution with ethanol, and a hydrophilic one by growing ZnO nanoparticles on the surface of different ceramic substrates used in construction, such as concrete, natural stone, or roofing tiles and ceramic tiles. The aim was to change the surface energy of the substrates and generate hierarchical roughness using the spray-coating technique.

The ceramic substrates were purchased locally and the concrete was prepared with sand and Portland cement. All substrates were washed and dried beforehand to remove any dirt or dust on the surface.

The modification in the hydrophobicity of the workpieces after the coatings were applied was determined by measuring the contact angle with a Dataphysics OCA 15 PLUS measuring device, using 3µl de-ionised water on the surfaces of the coated and uncoated pieces.

Fourier transform infrared spectroscopy (FT-IR) was used to analyse the changes in the bonds on the surface of the SiO<sub>2</sub> particles and the coated substrates.

Pull-off adhesion tests were carried out using an Elcometer 510 model T with a pull-off rate of 0.2 MPa/s and a 20mm pull stub on both coated and uncoated specimens with a surface area of 5 cm x 5 cm.

The morphology of the deposited particles was characterised using a JEOL 6010 Plus Scanning Electron Microscope with low vacuum configuration.

### 3. RESULTS AND DISCUSSION

#### 3.1. CONTACT ANGLE

Figure 1 shows images of the contact angle for the ceramic pieces both before and after the hydrophilic and hydrophobic coatings were applied. Figure 1a shows the ceramic tile material with an initial contact angle of  $72.8^\circ$  located in the centre of the image. On the far left, the contact angle with the hydrophilic coating is seen, with a value of  $17.8^\circ$ , while on the right side, the contact angle for the hydrophobic coating is shown, which reaches  $130^\circ$ .

Figures 1b and 1c show the contact angles for natural stone and concrete, respectively. Both materials had contact angles before the coatings were applied of  $52^\circ$  and  $55^\circ$ , respectively. Those values went down to  $22.4^\circ$  and  $30.9^\circ$  with the hydrophilic coating and up to  $144^\circ$  and  $145^\circ$  with the hydrophobic coating, respectively.

Figure 1d presents the contact angle for the roofing tile material. Before the coatings were applied, this material had an initial contact angle of  $97^\circ$ . With the hydrophilic coating, contact angle decreased to  $34^\circ$ , while with the hydrophobic coating, it increased to  $146^\circ$ .

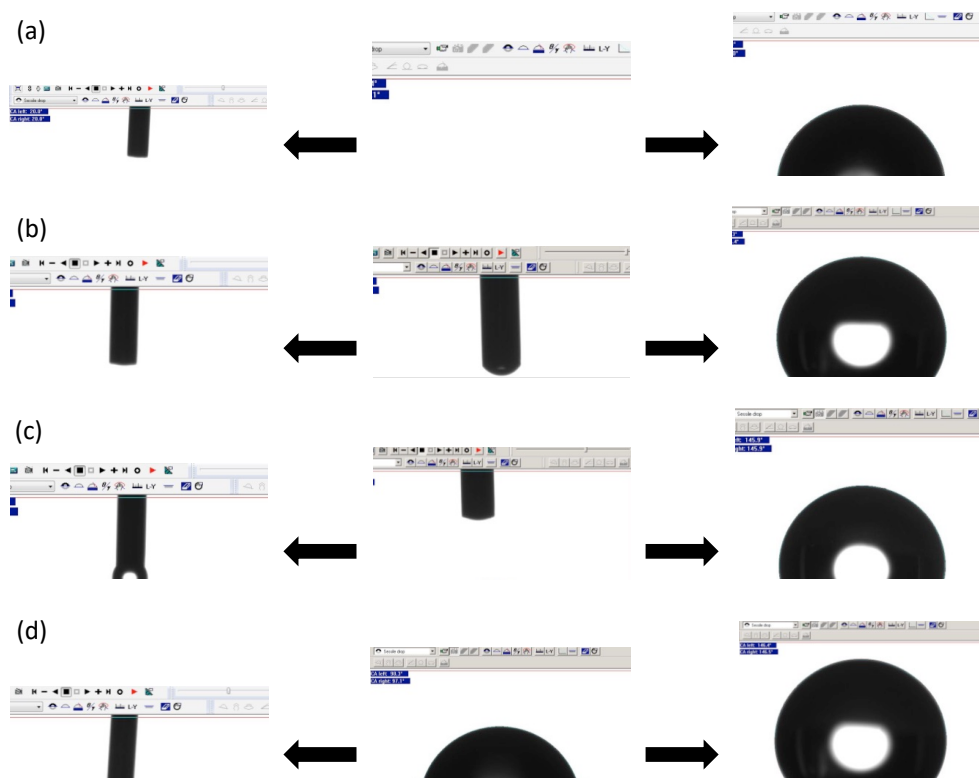


**Figure. 1.** Photos of the contact angle for the different test substrates a) ceramic tile, b) natural stone, c) concrete and d) roofing tile.

Although contact angles do not reach super-hydrophobic levels nor are they low enough to be considered super-hydrophilic, they do allow water droplets to move over the surface of the materials. In the case of the hydrophobic coating, the droplet may run a little thanks to the slight slope, whereas with the hydrophilic coating, the droplet spreads evenly over the surface, as expected.

### 3.2. ASSESSMENT OF COATING ADHESION

This evaluation compared the results obtained for coated and uncoated pieces. Figure 2a illustrates the set-up used for the adhesion test, which consists of a pull stub, resin and a coated substrate. Figure 2b shows the types of failures observed on the surface of the pull stub after the adhesion test.

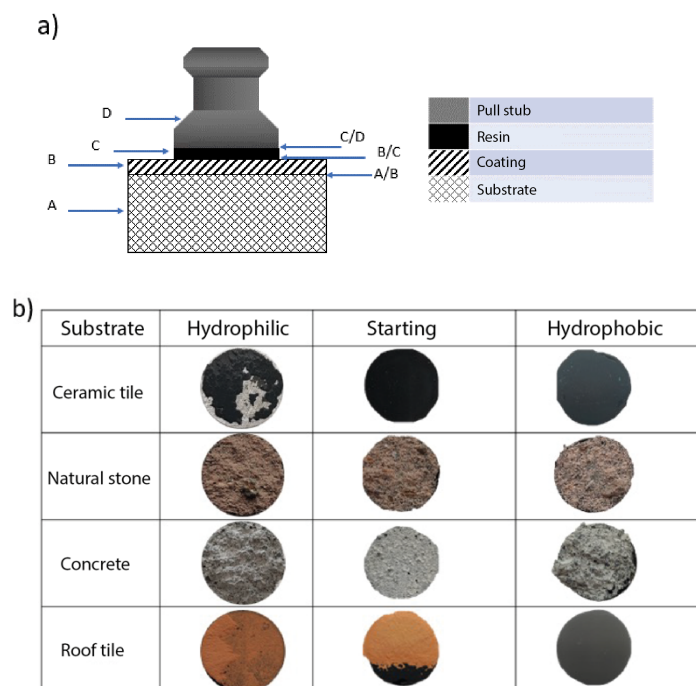


**Figure 2.** a) Diagram of the set-up for pull-off adhesion testing, b) bottom view of the pull stub after failure.

When the adhesion failure values presented in Figure 3 are analysed in conjunction with the images of the pull stub surface, one can see that, in the case of the hydrophobic covering, there was a decrease in the strength recorded for the ceramic tile and roofing tile materials. In these cases, failures occurred at the interface involving the coating. Consequently, average bond strength for the hydrophobic coating on those materials is estimated to be in the range of 3-3.5 MPa. On the other hand, when evaluating the natural stone and concrete materials with the hydrophobic coating, a slight increase in values was noted compared to the uncoated pieces. Furthermore, in Figure 2, it can be seen that failure was related to the cohesion of the substrate rather than the adhesion of the coating.

On the other hand, the results for the hydrophilic coating are also presented. Both the values in Figure 3 and the types of failure observed for the natural stone, concrete and roof tile materials (Figure 2a) were similar to those of the uncoated pieces. However, in the case of the tile, an increase in bond strength was seen and the type of failure observed occurred between the resin used and the pull stub. This behaviour might be related to the presence of ZnO microstructures on the smooth surface of the tile.

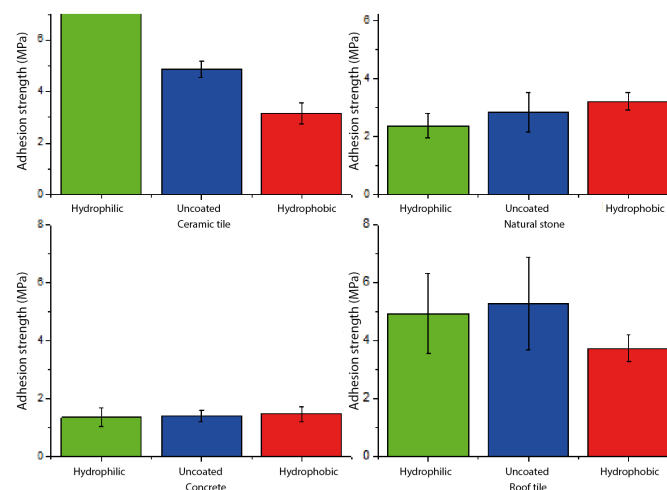


**Figure. 3.** Adhesion strength values recorded at failure for the different test substrates.

### 3.3. SCANNING ELECTRON MICROSCOPY

Scanning electron microscopy images were used in the study to evaluate the changes in surface morphology. Figure 4 presents a comparison between uncoated concrete surfaces and the same surfaces with hydrophobic and hydrophilic coatings.

Figure 4b shows an image of an uncoated concrete piece at a magnification of 50,000X, where a flat and smooth surface is visible. On the other hand, in (a) and (c), which are of concrete surfaces with hydrophilic and hydrophobic coatings, respectively, significant differences can be observed.

In (a), the hydrophilic coating is depicted, which was achieved by the deposition of two solutions. The first solution was used to seed the ZnO, while the second one was used to grow the ZnO nanorods. In the image, rod-shaped structures can be identified in the centre-left area. However, it is important to note that the size of those structures is rather large to be termed “nano”. Furthermore, one can see that growth of the structures was not uniform across the entire surface.

In (c), amorphous SiO<sub>2</sub> particles can be seen deposited on the surface of the concrete. Also present are clusters of those particles, which produce a non-uniform coating. That in turn creates areas on the concrete surface that are exposed to interaction with the droplets of water, leading to a decrease in the contact angle observed.

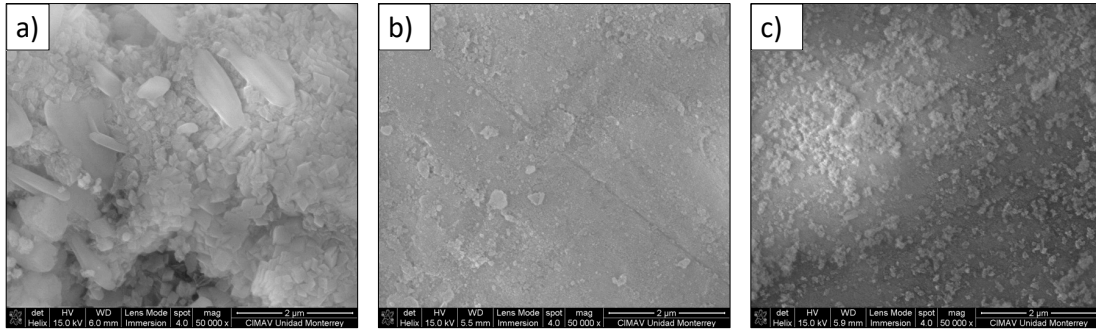


**Figure. 4.** Micrographs of the concrete surface a) with hydrophilic (ZnO) coating, b) with no coating, c) with hydrophobic coating (SiO<sub>2</sub>).

A future objective is to reduce the size of the deposited particles by making a ZnO seeding solution, which will permit more orderly growth and smaller-sized structures on the surface of the material. This approach aims to achieve greater uniformity and control of surface morphology, which could have a significant impact on the performance of the coating.



### 3.4. FOURIER TRANSFORM INFRARED SPECTROSCOPY

Functional group analyses were performed on the surface of  $\text{SiO}_2$  particles using Fourier transform infrared spectroscopy (FT-IR). Two sets of FT-IR spectra were obtained: the first corresponding to test substrates before any coating was applied, and the second to the substrates after the hydrophobic coating was applied. The spectra are presented in Figure 5.

The top three spectra correspond to the roofing tile, natural stone and concrete substrates before coating, respectively. The bottom three spectra correspond to the same substrates with the hydrophobic ( $\text{SiO}_2$ ) coating.

In the spectra for coated natural stone and concrete pieces, characteristic bands of symmetric and asymmetric stretching vibrations can be identified for groups C-H in the  $2900\text{--}2850\text{ cm}^{-1}$  range [25]. Also, peaks corresponding to C-H bending vibrations are found in the  $1400\text{--}1350\text{ cm}^{-1}$  range, indicating the presence of the aliphatic TOS silane group on the surface of the materials [26]. Note the band located at  $807\text{ cm}^{-1}$ , assigned to the Si-C bond, which is formed as a result of the aliphatic group bond with the silicon of the TOS [27]. In addition, bands can be seen at  $972$  and  $456\text{ cm}^{-1}$ , corresponding to Si-OH and Si-O-Si, respectively [13], [28]. This increased intensity of the Si-O-Si bands can be attributed to the bonds generated on the surface of the  $\text{SiO}_2$  particles during the TOS coupling process.

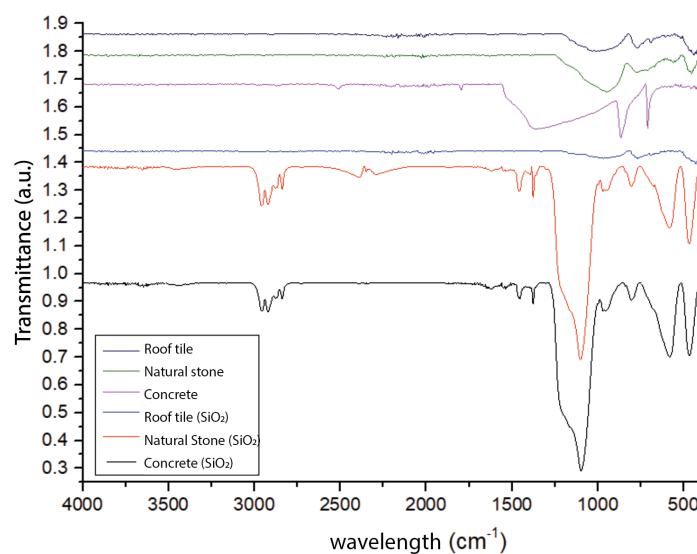


**Figure. 5.** FT-IR spectra of the test substrates before and after applying the hydrophobic  $\text{SiO}_2$  coating.



## 4. CONCLUSIONS

The coatings developed in this project enable the affinity of water to be modified on the surface of various ceramic substrates used in construction. These coatings, based on  $\text{SiO}_2$  and  $\text{ZnO}$  nanoparticles, have demonstrated their ability to alter the surface roughness and surface energy of the materials, resulting in significant changes in contact angles and an ability to repel or retain water.

Our results revealed that hydrophobic coatings can generate contact angles greater than  $130^\circ$ , indicating high water repellency, while hydrophilic coatings can reduce contact angles to less than  $35^\circ$ , thus enhancing water affinity. Although these values do not reach super-hydrophobic or super-hydrophilic extremes, they demonstrate the effectiveness of the coatings in modifying surface properties in a controlled manner.

In terms of coating adhesion, a variation in performance was observed, depending on the type of material and the type of coating. In general, hydrophobic coatings exhibited a decrease in adhesion strength on materials such as ceramic tiles and roofing tiles. On the other hand, hydrophilic coatings did not significantly affect adhesion on most substrates, except for the ceramic tile, where an increase in adhesion strength was observed.

Using scanning electron microscopy, it was possible to visualise the differences in surface morphology before and after the coatings were applied. Although the morphology was modified by the nanoparticle deposition, the need to improve uniformity and control growth of the structures on the surface of the substrates is a major factor.

Finally, Fourier transform infrared spectroscopy confirmed the presence of functional groups on the surface of the  $\text{SiO}_2$  particles after the TOS coupling process.

The findings presented here support the possibility of extending the lifespan of buildings, preserving cultural heritage and reducing maintenance costs, while contributing to a better understanding of surface modification in practical applications.

## 5. REFERENCES

- [1] M. Ricca *et al.*, "Building materials and decay assessment of the Gerace Cathedral (Reggio Calabria, Southern Italy)," *Case Studies in Construction Materials*, vol. 19, Dec. 2023, doi: 10.1016/j.cscm.2023.e02225.
- [2] T. T. Awasho and S. K. Alemu, "Assessment of public building defects and maintenance practices: Cases in Mettu town, Ethiopia," *Heliyon*, vol. 9, no. 4, Apr. 2023, doi: 10.1016/j.heliyon.2023.e15052.
- [3] N. Prieto-Taboada *et al.*, "The potential of in situ Raman spectroscopy in the study of the health of cement-based materials of modern buildings during restoration works," *Journal of Raman Spectroscopy*, vol. 52, no. 11, pp. 1868–1877, Nov. 2021, doi: 10.1002/jrs.6217.
- [4] X. Wang, J. P. Nshimiyimana, D. Huang, X. Diao, and N. Zhang, "Durable superhydrophilic and antireflective coating for high-performance anti-dust photovoltaic systems," *Applied Nanoscience (Switzerland)*, vol. 11, no. 3, pp. 875–885, 2021, doi: 10.1007/s13204-020-01643-0.
- [5] X. Wang *et al.*, "Preparation of a temperature-sensitive superhydrophobic self-cleaning SiO<sub>2</sub>-TiO<sub>2</sub>@PDMS coating with photocatalytic activity," *Surf Coat Technol*, vol. 408, no. July 2020, p. 126853, 2021, doi: 10.1016/j.surfcoat.2021.126853.
- [6] M. Janus and K. Zajac, "Self-cleaning efficiency of nanoparticles applied on facade bricks," *Nanotechnology in Eco-efficient Construction: Materials, Processes and Applications*, pp. 591–618, 2018, doi: 10.1016/B978-0-08-102641-0.00024-4.
- [7] R. Zarzuela *et al.*, "Multifunctional silane-based superhydrophobic/impregnation treatments for concrete producing C-S-H gel: Validation on mockup specimens from European heritage structures," *Constr Build Mater*, vol. 367, Feb. 2023, doi: 10.1016/j.conbuildmat.2022.130258.
- [8] W. Liu *et al.*, "Make the building walls always clean: A durable and anti-bioadhesive diatomaceous earth@SiO<sub>2</sub> coating," *Constr Build Mater*, vol. 301, no. April, p. 124293, 2021, doi: 10.1016/j.conbuildmat.2021.124293.
- [9] O. Saucedo Orozco, "Estudio de la Mejora del Método de Ogihara en la Generación de Nanopartículas de SiO<sub>2</sub> para el Desarrollo de Superhidrofobicidad en Diferentes Sustratos Cerámicos," Universidad Autónoma de Nuevo León, 2021.
- [10] I. F. Wahab, A. R. Bushroa, S. Wee Teck, T. T. Azmi, M. Z. Ibrahim, and J. W. Lee, "Fundamentals of antifogging strategies, coating techniques and properties of inorganic materials; a comprehensive review," *Journal of Materials Research and Technology*, vol. 23, Elsevier Editora Ltda, pp. 687–714, Mar. 01, 2023, doi: 10.1016/j.jmrt.2023.01.015.
- [11] W. Yao, J. Qin, Y. Chen, L. Wu, B. Jiang, and F. Pan, "SiO<sub>2</sub> nanoparticles-containing slippery-liquid infused porous surface for corrosion and wear resistance of AZ31 Mg alloy," *Mater Des*, vol. 227, Mar. 2023, doi: 10.1016/j.matdes.2023.111721.
- [12] T. Liang *et al.*, "Corrosion inhibition effect of nano-SiO<sub>2</sub> for galvanized steel superhydrophobic surface," *Surf Coat Technol*, vol. 406, no. November, p. 126673, 2021, doi: 10.1016/j.surfcoat.2020.126673.
- [13] X. Yu, X. Liu, X. Shi, Z. Zhang, H. Wang, and L. Feng, "SiO<sub>2</sub> nanoparticle-based superhydrophobic spray and multi-functional surfaces by a facile and scalable method," *Ceram Int*, vol. 45, no. 12, pp. 15741–15744, 2019, doi: 10.1016/j.ceramint.2019.05.014.
- [14] C. Kallweit, M. Bremer, D. Smazna, T. Karrock, R. Adelung, and M. Gerken, "Photoresponsive hierarchical ZnO-PDMS surfaces with azobenzene-polydopamine coated nanoparticles for reversible wettability tuning," *Vacuum*, vol. 146, pp. 386–395, 2017, doi: 10.1016/j.vacuum.2017.03.023.
- [15] H. Qin, H. Zhou, W. Guo, F. Yan, and H. Xiao, "Reversal of wettability of carbon cloth by microwave-assisted modification technology for efficient oil-water separation application," *Surf Coat Technol*, vol. 419, no. May, p. 127260, 2021, doi: 10.1016/j.surfcoat.2021.127260.
- [16] F. D. Rodríguez Villalobos, "Estudio y Mejoramiento del Método de Generación por Sol-Spray de un Recubrimiento Superhidrofílico para el Desarrollo de Superficies Cerámicas Autolimpiables," Universidad Autónoma de Nuevo León, 2018.
- [17] D. Siang Ng *et al.*, "Influence of SiO<sub>2</sub>, TiO<sub>2</sub> and Fe<sub>2</sub>O<sub>3</sub> nanoparticles on the properties of fly ash blended cement mortars," *Constr Build Mater*, vol. 258, 2020, doi: 10.1016/j.conbuildmat.2020.119627.
- [18] M. Jacobs, Y. De Vos, and V. Middelkoop, "Thickness controlled SiO<sub>2</sub>/TiO<sub>2</sub> sol-gel coating by spraying," *Open Ceramics*, vol. 6, no. December 2020, pp. 0–7, 2021, doi: 10.1016/j.oceram.2021.100121.
- [19] M. Dell'Edera *et al.*, "Photocatalytic TiO<sub>2</sub>-based coatings for environmental applications," *Catal Today*, no. May, 2021, doi: 10.1016/j.cattod.2021.04.023.
- [20] J. M. Shockley, S. Descartes, P. Vo, E. Irissou, and R. R. Chromik, "The influence of Al<sub>2</sub>O<sub>3</sub> particle morphology on the coating formation and dry sliding wear behavior of cold sprayed Al-Al<sub>2</sub>O<sub>3</sub> composites," *Surf Coat Technol*, vol. 270, pp. 324–333, 2015, doi: 10.1016/j.surfcoat.2015.01.057.
- [21] H. Ogihara, J. Xie, and T. Saji, "Factors determining wettability of superhydrophobic paper prepared by spraying nanoparticle suspensions," *Colloids Surf A Physicochem Eng Asp*, vol. 434, pp. 35–41, 2013, doi: 10.1016/j.colsurfa.2013.05.034.
- [22] X. Zhao *et al.*, "Environmentally benign and durable superhydrophobic coatings based on SiO<sub>2</sub> nanoparticles and silanes," *J Colloid Interface Sci*, vol. 542, pp. 8–14, 2019, doi: 10.1016/j.jcis.2019.01.115.

- [23] Talinungsang, D. Upadhaya, P. Kumar, and D. D. Purkayastha, "Superhydrophilicity of photocatalytic ZnO/SnO<sub>2</sub> heterostructure for self-cleaning applications," *J Solgel Sci Technol*, vol. 92, no. 3, pp. 575–584, 2019, doi: 10.1007/s10971-019-05127-8.
- [24] J. Li, Q. Sun, S. Han, J. Wang, Z. Wang, and C. Jin, "Reversibly light-switchable wettability between superhydrophobicity and superhydrophilicity of hybrid ZnO/bamboo surfaces via alternation of UV irradiation and dark storage," *Prog Org Coat*, vol. 87, pp. 155–160, 2015, doi: 10.1016/j.porgcoat.2015.05.028.
- [25] H. Y. Nah *et al.*, "Comparisional studies of surface modification reaction using various silylating agents for silica aerogel," *J Solgel Sci Technol*, vol. 96, no. 2, pp. 346–359, 2020, doi: 10.1007/s10971-020-05399-5.
- [26] B. Majhy, R. Iqbal, and A. K. Sen, "Facile fabrication and mechanistic understanding of a transparent reversible superhydrophobic – superhydrophilic surface," *Sci Rep*, vol. 8, no. 1, pp. 1–11, 2018, doi: 10.1038/s41598-018-37016-5.
- [27] B. Améduri, H. Koroniak, J. Wolska, A. Szwajca, and J. Walkowiak-Kulikowska, "Aromatic fluorocopolymers based on  $\alpha$ -(difluoromethyl)styrene and styrene: synthesis, characterization, and thermal and surface properties," *RSC Adv*, vol. 8, no. 73, pp. 41836–41849, 2018, doi: 10.1039/c8ra09340g.
- [28] A. Tombesi *et al.*, "Aerosol-assisted chemical vapour deposition of transparent superhydrophobic film by using mixed functional alkoxysilanes," no. October 2018, pp. 1–12, 2019, doi: 10.1038/s41598-019-43386-1.